

Perceptual Learned Video Compression with Recurrent Conditional GAN

Ren Yang, Luc Van Gool, Radu Timofte

Computer Vision Laboratory, D-ITET, ETH Zurich, Switzerland
 {ren.yang, vangool, radu.timofte}@vision.ee.ethz.ch

Abstract

This paper proposes a Perceptual Learned Video Compression (PLVC) approach with recurrent conditional generative adversarial network. In our approach, the recurrent auto-encoder-based generator learns to fully explore the temporal correlation for compressing video. More importantly, we propose a recurrent conditional discriminator, which judges raw and compressed video conditioned on both spatial and temporal information, including the latent representation, temporal motion and hidden states in recurrent cells. This way, in the adversarial training, it pushes the generated video to be not only spatially photo-realistic but also temporally consistent with groundtruth and coherent among video frames. The experimental results show that the proposed PLVC model learns to compress video towards good perceptual quality at low bit-rate, and outperforms the previous traditional and learned approaches on several perceptual quality metrics. The user study further validates the outstanding perceptual performance of PLVC in comparison with the latest learned video compression approaches and the official HEVC test model (HM 16.20). The codes will be released at <https://github.com/RenYang-home/PLVC>.

Introduction

The past decade has witnessed the increasing popularity of video streaming over the Internet (Cisco 2020). The quantities of high quality and high resolution videos are also rapidly increasing. Therefore, video compression is essential to enable the efficient video transmission over the band-limited Internet. In recent years, inspired by the success of learning-based image compression, plenty of end-to-end learned video compression approaches were proposed (Xu et al. 2020). The performance of the state-of-the-art has shown the promising future of learned compression. Nevertheless, most existing approaches are only optimized towards distortion, *i.e.*, PSNR and MS-SSIM, without considering the *perceptual* quality of compressed image and video. Most recently, Generative Adversarial Network (GAN) has been used in image compression towards perceptual quality (Agustsson et al. 2019; Mentzer et al. 2020).

However, the study on perceptual learned *video* compression still remains blank. Different from image compression,

Copyright © 2022, Association for the Advancement of Artificial Intelligence (www.aaai.org). All rights reserved.

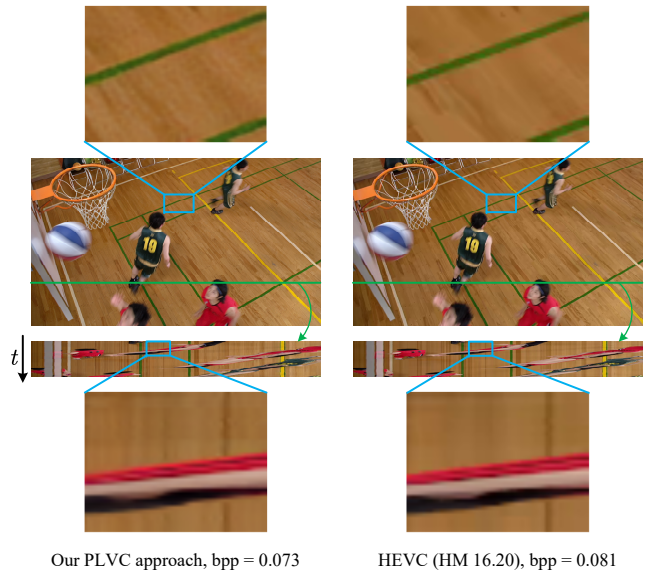


Figure 1: Example of the proposed PLVC approach in comparison with the official HEVC test model (HM 16.20).

generative video compression is a more challenging task. If simply borrowing the independent GAN of image compression to video, each frame is learned to be generated independently without temporal constraint, as the discriminator only pushes the spatial perceptual quality without considering temporal coherence. This may lead to the incoherent motion among video frames and thus the temporal flickering may severely degrade the perceptual quality.

To overcome these challenges, we propose a Perceptual Learned Video Compression (PLVC) approach with recurrent conditional GAN, which consists of a recurrent generator and a recurrent conditional discriminator. The recurrent generator contains recurrent auto-encoders for video compression, and learns to reconstruct visually pleasing compressed video in the adversarial training. More importantly, we propose a recurrent conditional discriminator, which judges raw and compression video conditioned on the spatial-temporal information, including latent representations, motion and the hidden states transferred through recurrent cells. Therefore, in the adversarial training, the dis-

criminator is able to force the recurrent generator to reconstruct photo-realistic and also temporally coherent video.

Figure 1 shows the visual result of the proposed PLVC approach on *BasketballDrill* (bpp = 0.0730) in comparison with the official HEVC test model HM 16.20 (bpp = 0.0813). The top of Figure 1 shows that our PLVC approach achieves richer and more photo-realistic textures than HEVC. At the bottom of Figure 1, we show the temporal profiles by vertically stacking a specific row (marked as green) along time steps. It can be seen that the result of our PLVC approach has comparable temporal coherence with HEVC but has more detailed textures. As a result, we outperform HEVC on the perceptual quality at lower bit-rate. The contribution of this paper are summarized as:

- We propose a novel perceptual video compression approach with recurrent conditional GAN, which learns to compress video and generate photo-realistic and temporally coherent compressed frames.
- We propose the adversarial loss functions for perceptual video compression to balance the bit-rate, distortion and perceptual quality.
- The experiments (including user study) show the outstanding perceptual performance of our PLVC approach in comparison with the latest learned and traditional video compression approaches.
- The ablation studies show the effectiveness of the adversarial training and the temporal conditions in our approach.

Related work

Learned image compression. In the past a few years, learned image compression has been attracting increasing interest. For instance, Ballé *et al.* proposed utilizing the variational auto-encoder for deep image compression and proposed the factorized (Ballé, Laparra, and Simoncelli 2017) and hyperprior (Ballé *et al.* 2018) entropy models. Later, the auto-regressive entropy models (Minnen, Ballé, and Toderici 2018; Mentzer *et al.* 2018; Lee, Cho, and Beack 2019; Cheng *et al.* 2019; He *et al.* 2021) were proposed to improve the compression efficiency. Recently, the coarse-to-fine model (Hu, Yang, and Liu 2020) and the wavelet-like deep auto-encoder (Ma *et al.* 2020) were designed to further advance the rate-distortion performance, and successfully outperform the latest traditional image coding standard BPG (Bellard 2018). Besides, there are also the methods with RNN-based auto-encoder (Toderici *et al.* 2016, 2017; Johnston *et al.* 2018) or conditional auto-encoder (Choi, El-Khany, and Lee 2019) for variable rate compression. Moreover, Agustsson *et al.* (2019) and Menzter *et al.* (2020) proposed applying GAN for perceptual image compression to achieve photo-realistic compressed images at low bit-rate. They show the great potential of utilizing generative model for perceptual video compression.

Learned video compression. Inspired by above works, a great number of end-to-end learned video compression methods have been proposed. In 2018, a deep video compression method through image interpolation (Wu, Singhal, and Krahenbuhl 2018) was proposed. Then, an end-

to-end learned video compression method, called DVC (Lu *et al.* 2019) was proposed in 2019. The DVC method uses optical flow for motion estimation, and utilizes two auto-encoders to compress the motion and residual, respectively. Later, the M-LVC method (Lin *et al.* 2020) extends the range of reference frames and beats the DVC baseline. Meanwhile, a plenty of learned video compression methods with bi-directional prediction (Djelouah *et al.* 2019), one-stage flow (Liu *et al.* 2020), hierarchical layers (Yang *et al.* 2020), scale-space flow (Agustsson *et al.* 2020) and resolution-adaptive flow coding (Hu *et al.* 2020) were proposed. Besides, the content adaptive and error propagation aware model (Lu *et al.* 2020) and the resolution-adaptive flow coding (Hu *et al.* 2020) strategy were employed for improving the compression efficiency. Most recently, the recurrent frameworks (Golinski *et al.* 2020; Yang *et al.* 2021) were adopted to adequately make use of temporal information in a large range of frames for better video compression. However, all above methods are optimized for PSNR or MS-SSIM. The generative video compression towards perceptual quality still remains blank and is to be studied.

Preliminary

GAN and conditional GAN. GAN was first introduced by Goodfellow *et al.* (Goodfellow *et al.* 2014) for image generation. It generates photo-realistic images (x) by optimizing the adversarial loss

$$\min_G \max_D \mathbb{E}[f(D(x))] + \mathbb{E}[g(D(G(y)))], \quad (1)$$

where f and g are scalar functions, and G maps the prior y to p_x . We define $\hat{x} = G(y)$, and then the discriminator D learns to distinguish \hat{x} from x . In the adversarial training, it pushes the distribution of generated samples $p_{\hat{x}}$ as similar to p_x as possible to fool D . As such, G is able to generate photo-realistic images.

Later, the conditional GAN (Mirza and Osindero 2014) was proposed to generate images *conditional* on prior information. Defining the conditions as c , the loss function can be expressed as

$$\min_G \max_D \mathbb{E}[f(D(x|c))] + \mathbb{E}[g(D(\hat{x}|c))] \quad (2)$$

with $\hat{x} = G(y)$. The goal of employing c in (2) is to push G to generate $\hat{x} \sim p_{\hat{x}|c}$ with the *conditional* distribution tending to be the same as $p_{x|c}$. In another word, it learns to fool D to believe that \hat{x} and x correspond to a shared prior c with the same conditional probability. By properly setting the condition prior c , the conditional GAN is expected to have the potential to generate frames with desired properties, *e.g.*, rich texture, temporal consistency and coherence, *etc.* This motivates us to propose a conditional GAN for perceptual video compression.

Proposed PLVC approach

Figure 2 shows the framework of the proposed PLVC approach with recurrent conditional GAN, which contains a recurrent generator (G) and a recurrent conditional discriminator (D). Specifically, for compressing the i -th frame x_i ,

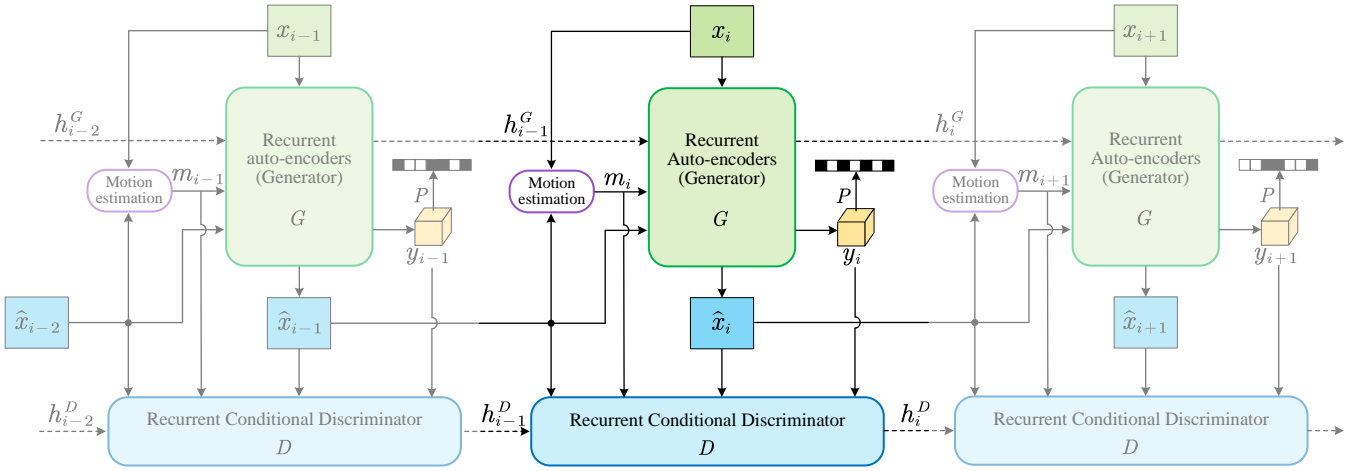


Figure 2: The proposed PLVC approach with recurrent GAN, which includes a recurrent generator G and a recurrent conditional discriminator D . The dash lines indicate the temporal information transferred through the recurrent cells in G and D . Additionally, D takes y_i and m_i as spatial-temporal conditions. $(\hat{x}_i, \hat{x}_{i-1})$ and (x_i, x_{i-1}) are the compressed and raw samples to be distinguished by D .

we first estimate the motion m_i between x_i and its previously compressed frame \hat{x}_{i-1} by the pyramid optical flow network (Ranjan and Black 2017). Then, the recurrent generator G takes \hat{x}_{i-1} and m_i as inputs to compress the current frame x_i to (quantized) latent representation y_i and generate the compressed frame \hat{x}_i . The y_i is then encoded into bit-stream by the probability function estimated by a learned entropy model P .

The discriminator D is designed with a recurrent structure, and learns to discriminate raw and compressed videos conditioned on the shared spatial-temporal features, including the spatial prior (y_i), short-term temporal prior (m_i) and long-term temporal prior (recurrent hidden states h_{i-1}^D). This way, in the adversarial training, the compressed video tends to have the same spatial-temporal features as the raw video, and therefore, the proposed PLVC approach achieves both spatially photo-realistic and temporally coherent compressed video. To train the proposed model towards perceptual video compression, we use the loss function which combines the rate-distortion loss and the adversarial loss. The architectures of G and D and the training strategies are introduced in the following.

Recurrent generator

Figure 3 illustrates the architecture of the recurrent generator G . Specifically, we first utilize a recurrent auto-encoder (Yang et al. 2021) to compress the motion map m_i . The auto-encoder generates the quantized latent representation y_i^m , and the compressed motion is denoted as \hat{m}_i , which is used to warp the reference frame \hat{x}_{i-1} to compensate the temporal motion. Then, the warped frame, the compressed motion and the reference frame are fed into a CNN, which increases the non-linearity of motion compensation and learns to refine the warped frame. We define the output of the CNN as the motion-compensated frame x'_i , and then another recurrent auto-encoder is applied to compress

the residual information $r_i = x_i - x'_i$. The latent representation of residual is defined as y_i^r , and \hat{r}_i denotes the compressed residual. Finally, we add \hat{r}_i to x'_i to obtain the compressed frame \hat{x}_i . The latent representations y_i^m and y_i^r are concatenated as y_i , which is encoded into a bitstream by the RPM (Yang et al. 2021) entropy model (denoted as P).

In aforementioned networks, the recurrent auto-encoders make up the recurrent structure of G , which facilitates it to compress frames and reconstruct outputs based on temporal prior. As such, G has the potential to generate visually pleasing and temporally coherent frames. Defining all hidden information transferred through the recurrent cells as

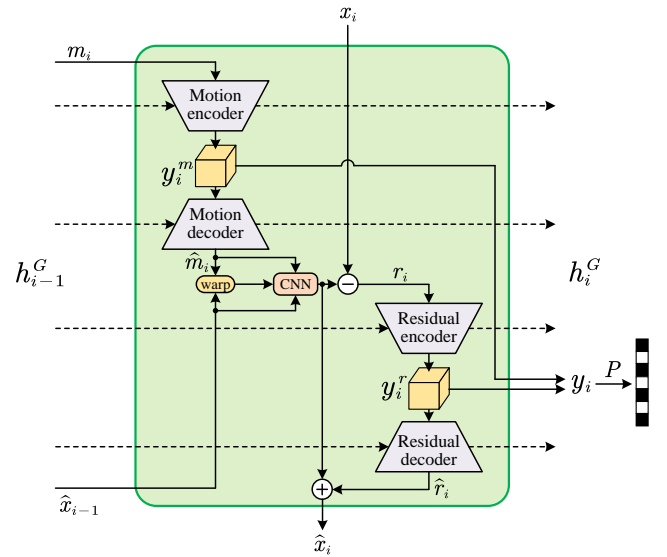


Figure 3: The architecture of the recurrent generator G . The dash lines are the hidden states of recurrent cells.

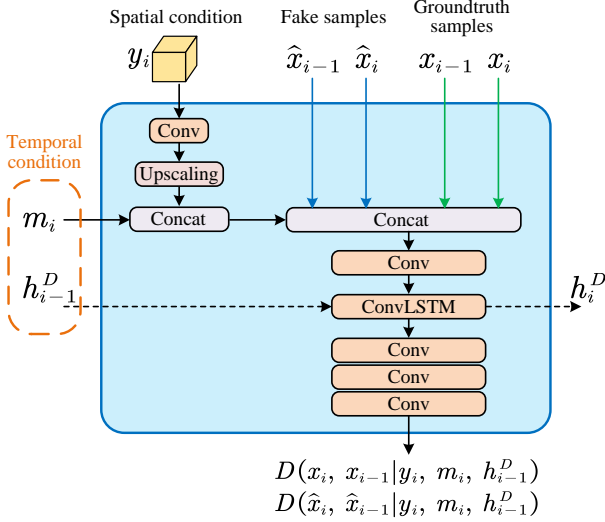


Figure 4: The architecture of the recurrent conditional discriminator D . Green and blue lines indicate the inputs of the groundtruth and compressed samples, respectively. The dash line is the hidden state transferred through recurrent cells.

h_i^G , the compressed frame and latent representation can be expressed as

$$\hat{x}_i, \mathbf{y}_i = G(\hat{x}_{i-1}, \mathbf{m}_i, x_i, h_{i-1}^G). \quad (3)$$

The more detailed architecture of each network in G is introduced in the *Supplementary Material*.

Recurrent conditional discriminator

Figure 4 shows the architecture of proposed recurrent conditional discriminator D . First, we follow (Mentzer et al. 2020) to feed \mathbf{y}_i as the spatial condition to D . This way, D learns to distinguish the groundtruth and compressed frames based on the shared spatial feature \mathbf{y}_i , and therefore pushes G to generate \hat{x}_i with similar spatial feature to x_i . It ensures the fidelity of \hat{x}_i .

More importantly, the temporal coherence is essential for visual quality. We insert a ConvLSTM layer in D to recurrently transfer the temporal information along time steps. The hidden state h_i^D can be seen as a long-term temporal condition fed to D , facilitating D to recurrently discriminate raw and compressed video taking temporal coherence into consideration. Furthermore, it is necessary to consider the temporal fidelity in video compression, *i.e.*, we expect the motion between compressed frames is consistent with that between raw frames. For example, the ball moves along the same path in the videos before and after compression. Hence, we propose D to take as inputs the frame pairs (x_i, x_{i-1}) and $(\hat{x}_i, \hat{x}_{i-1})$ and make the judgement based on the same motion vectors \mathbf{m}_i as the short-term temporal condition. If without the condition of \mathbf{m}_i , G may learn to generate photo-realistic $(\hat{x}_i, \hat{x}_{i-1})$ but with incorrect motion between the frame pair. This leads to the poor temporal fidelity to the groundtruth video. It motivates us to include the temporal condition \mathbf{m}_i as an input to the discriminator.

Table 1: The hyper-parameters for training PLVC models.

Quality	R_T (bpp)	λ	α_1	α_2	λ'	β
Low	0.025	256	3.0	0.010	100	0.1
Medium	0.050	512	1.0	0.010	100	0.1
High	0.100	1024	0.3	0.001	100	0.1

Besides, the ablation study also indicates that during the optimization of recurrent adversarial loss, the condition \mathbf{m}_i is also effective to improve the coherence of sequential frames.

Given these conditions, we have $\mathbf{c} = [\mathbf{y}_i, \mathbf{m}_i, h_{i-1}^D]$ in (2) in our PLVC approach. The output of D can be formulated as $D(x_i, x_{i-1} | \mathbf{y}_i, \mathbf{m}_i, h_{i-1}^D)$ and $D(\hat{x}_i, \hat{x}_{i-1} | \mathbf{y}_i, \mathbf{m}_i, h_{i-1}^D)$ for raw and compressed samples, respectively. When optimizing the recurrent conditional adversarial loss on sequential frames, the compressed video $\{\hat{x}_i\}_{i=1}^T$ tends to have the same spatial-temporal feature as the raw video $\{x_i\}_{i=1}^T$. As such, we achieve perceptual video compression with temporally coherent and spatially photo-realistic frames. Please refer to the *Supplementary Material* for the detailed architecture of each network in D .

Training strategies

Our PLVC model is trained on the Vimeo-90k (Xue et al. 2019) dataset. In each sample, the first frame is compressed as an I-frame, using the latest generative image compression approach (Mentzer et al. 2020). Other 6 frames are P-frames. To train the proposed network, we first warm up G on the first P-frame (x_i) by the rate-distortion loss

$$\mathcal{L}_w^1 = R(\mathbf{y}_1) + \lambda \cdot d(\hat{x}_1, x_1). \quad (4)$$

In (4), $R(\cdot)$ denotes the bit-rate estimated by the RPM (Yang et al. 2021) entropy model, and we use the Mean Square Error (MSE) as the distortion term d . Besides, λ is the hyper-parameter to balance the rate and distortion terms. After the convergence of (4), we further warm up G on consecutive P-frames by optimizing the rate-distortion loss

$$\mathcal{L}_w = \sum_{i=1}^N R(\mathbf{y}_i) + \lambda \cdot d(\hat{x}_i, x_i). \quad (5)$$

Then, we propose training D and G alternately with the loss function combining the rate-distortion loss and the non-saturating (Lucic et al. 2018) adversarial loss. Specifically, the loss functions are expressed as follows:

$$\begin{aligned} \mathcal{L}_D &= \sum_{i=1}^N \left(-\log(1 - D(\hat{x}_i, \hat{x}_{i-1} | \mathbf{y}_i, \mathbf{m}_i, h_{i-1}^D)) \right. \\ &\quad \left. - \log D(x_i, x_{i-1} | \mathbf{y}_i, \mathbf{m}_i, h_{i-1}^D) \right), \\ \mathcal{L}_G &= \sum_{i=1}^N \left(\alpha \cdot R(\mathbf{y}_i) + \lambda' \cdot d(\hat{x}, x) \right. \\ &\quad \left. - \beta \cdot \log D(\hat{x}_i, \hat{x}_{i-1} | \mathbf{y}_i, \mathbf{m}_i, h_{i-1}^D) \right). \end{aligned} \quad (6)$$

In (6), α , λ' and β are the hyper-parameters to control the trade-off of bit-rate, distortion and perceptual quality. We

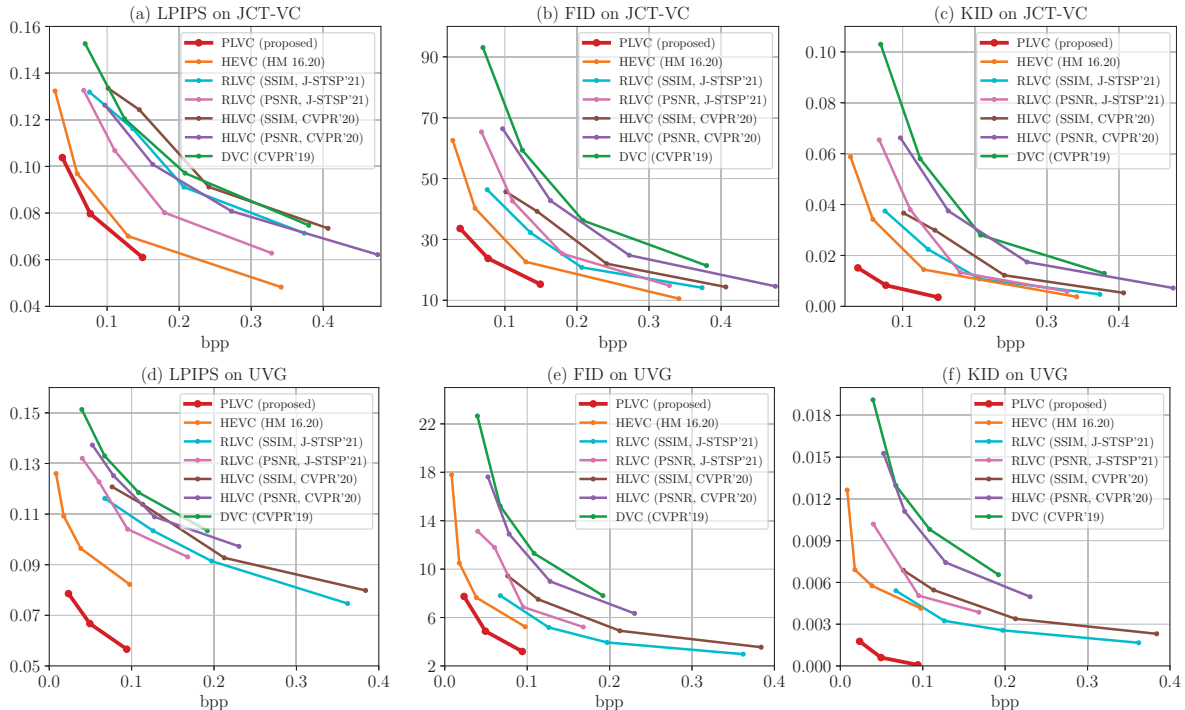


Figure 5: The numerical results on the UVG and JCT-VC datasets in terms of LPIPS, FID and KID.

set three target bit-rates R_T to easily control the operating points, and let $\alpha = \alpha_1$ when $R(\mathbf{y}_i) \geq R_T$, and $\alpha = \alpha_2 \ll \alpha_1$ when $R(\mathbf{y}_i) < R_T$. The hyper-parameters are shown in Table 1. Note that we set R_T relatively lower than non-generative methods. The reason is two-fold: 1) generative compression mainly aims at utilizing GAN to generate images/frames with good perceptual quality at low bit-rates (Agustsson et al. 2019); 2) our PLVC model trained with the highest R_T in Table 1 achieves comparable or better performance on perceptual metrics than the non-generative methods at their highest bit-rates, which are several times more than ours (see Figure 5).

Experiments

Settings

We follow the previous learned video compression approaches (Lu et al. 2019, 2020; Yang et al. 2020, 2021) to evaluate the performance on the JCT-VC (Bossen 2013) (Classes B, C and D) and the UVG (Mercat, Viitanen, and Vanne 2020) datasets. We compare the proposed PLVC approach with various video compression approaches. On perceptual metrics, we compare with the official HEVC test model (HM 16.20) and the latest open-sourced¹ learned video compression approaches DVC (Lu et al. 2019), HLVC (Yang et al. 2020) and RLVC (Yang et al. 2021). We also report our MS-SSIM and PSNR results in comparison with plenty of existing approaches.

¹Since the previous approaches do not report the results on perceptual metrics, we need to run the open-sourced codes to repro-

Numerical performance

Perceptual quality. To numerically evaluate the perceptual quality, we calculate the Learned Perceptual Image Patch Similarity (LPIPS) (Zhang et al. 2018), Fréchet Inception Distance (FID) (Heusel et al. 2017) and Kernel Inception Distance (KID) (Bińkowski et al. 2018) on our PLVC and compared approaches. LPIPS (Zhang et al. 2018) measures the distance in the feature space of DNN. FID (Heusel et al. 2017) and KID (Bińkowski et al. 2018) calculates the similarity between the distributions of the groundtruth and generated frames. These metrics have been validated to be effective for evaluating perceptual quality.

The results are shown in Figure 5. We observe that the proposed PLVC approach achieves good perceptual performance at low bit-rates, and outperforms all compared models in terms of all three perceptual metrics. Especially, our PLVC approach reaches comparable or even better LPIPS, FID and KID values than other approaches which are at $2\times$ to $4\times$ bit-rates of ours. It validates the effectiveness of the proposed method on compressing video with visually pleasing frames at low bit-rates.

Fidelity. Besides, we also compare the MS-SSIM and PSNR in Figure 7 to show the fidelity of our results. It can be seen from Figure 7 that the MS-SSIM of our PLVC approach is better than DVC (Lu et al. 2019) and comparable with Lu *et al.* (Lu et al. 2020). Our PSNR result also competes DVC (Lu et al. 2019). These verify that the proposed PLVC approach is able to maintain the fidelity to an acceptable de-

duce the compressed frames for perceptual evaluation.



Figure 6: The visual results of the proposed PLVC approach, HM 16.20 and the MS-SSIM-optimized RLVC (Yang et al. 2021).

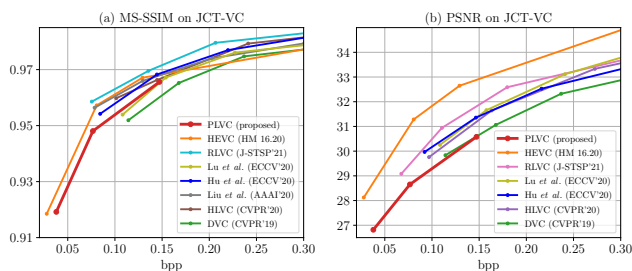


Figure 7: The MS-SSIM and PSNR results on JCT-VC.

gree when compressing video towards perceptual quality.

Visual results and user study

Figure 6 shows the visual results of the proposed PLVC approach in comparison with HM 16.20 and the latest learned video compression approach RLVC (Yang et al. 2021) (MS-SSIM optimized²). The top of Figure 6 illustrates the spatial textures, and the bottom shows the temporal profiles by vertically stacking a specific row along time steps. It can be seen from Figure 6 that the proposed PLVC approach achieves richer and more photo-realistic textures at lower bit-rates than the compared methods. Besides, the temporal profiles indicate that our PLVC approach maintains the comparable temporal coherence with the groundtruth in both slow motion (*PartyScene*, left in Figure 6) and fast motion (*RaceHorses*, right in Figure 6) videos. In conclusion, the proposed PLVC approach generates photo-realistic and coherent compressed videos, obviously advancing the perceptual quality of previous methods. More visual results are provided in the *Supplementary Material*.

We further conduct a MOS experiment with 12 subjects. The subjects are asked to rate the compressed videos with the score from 0 to 100 according to subjective quality. Higher score indicates better perceptual quality. The averaged rate-MOS curves on the JCT-VC dataset are shown in Figure 8. As we can see from Figure 8, our PLVC approach

²MS-SSIM (Wang, Simoncelli, and Bovik 2003) is more correlated to perceptual quality than PSNR.

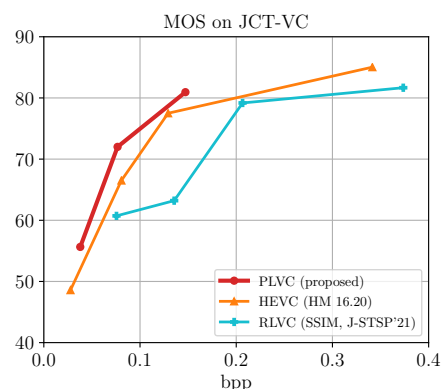


Figure 8: The rate-MOS result of the user study.

successfully outperforms the official HEVC test model HM 16.20, especially at low bit-rates, and we are significantly better than the MS-SSIM-optimized RLVC (Yang et al. 2021). We also provide video examples in the project page for a better comparison.

Ablation studies

Recall that the main contribution of the proposed approach is two fold: 1) we propose applying generative adversarial network for perceptual video compression; 2) we propose the recurrent conditional D to ensure the temporal coherence of compressed video. In ablation studies, we analyze the effectiveness of the generative adversarial network and the temporal conditions h_i^D and m_i .

We provide the ablation analyses in terms of LPIPS, and also conducted an ablation user study with 10 subjects to make the ablation study mode convincing. The performance of the ablation user study are shown as the MOS results in Figure 9. Moreover, we also provide example videos of ablation results in the *Supplementary Material*.

Generative adversarial network. We illustrate the results of the distortion-optimized PLVC model, denoted as PLVC (w/o GAN) in Figure 9, compared with the proposed PLVC approach. The model of PLVC (w/o GAN) is trained

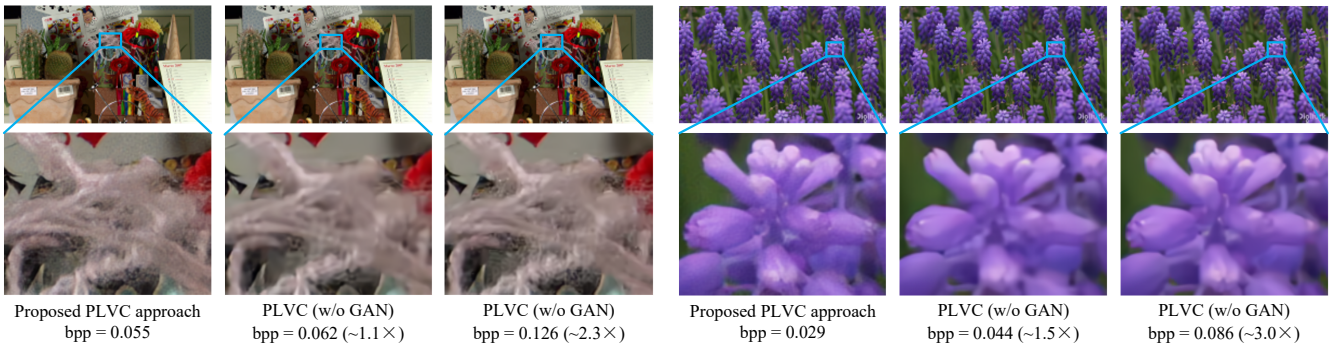


Figure 9: The ablation study on PLVC with and without GAN. (Zoom-in for better viewing)

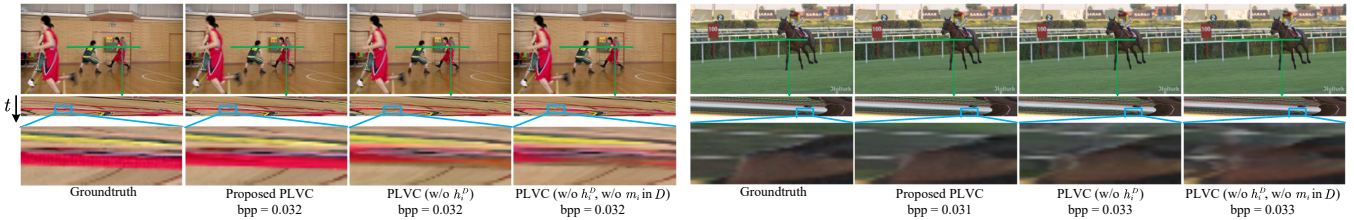


Figure 10: The temporal coherence of the ablation study on the temporal conditions h_i^D and m_i in D .

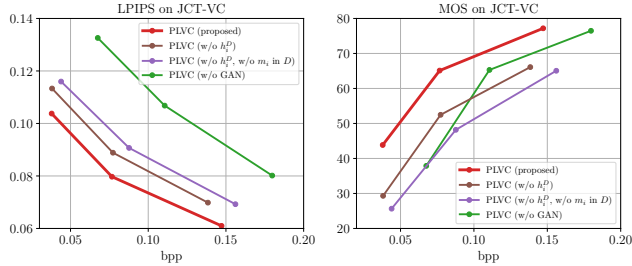


Figure 11: The LPIPS and MOS results of the ablation study. This MOS result is independent from Figure 8 with different subjects, so the MOS values can only be compared within each figure.

only until the convergence of (5) without the adversarial loss in (6). It can be seen from Figure 9 that the proposed PLVC approach achieves richer texture and more photo-realistic frames than PLVC (w/o GAN), even if when PLVC (w/o GAN) consumes $2\times$ to $3\times$ bit-rates. This is also verified by the LPIPS and MOS performance in Figure 11.

Temporal conditions in D . Then, we analyze the temporally conditional D . We first remove the recurrency in D , i.e., w/o h_i^D . As we can see from Figure 10, the temporal profile of PLVC (w/o h_i^D) (third column) is obviously distorted in comparison with the proposed PLVC approach and the groundtruth. As shown in Figure 11, the LPIPS and MOS performance of PLVC (w/o h_i^D) also degrades in comparison with the proposed PLVC model. Then, we further remove the temporal condition m_i from D and denote it as PLVC (w/o h_i^D , w/o m_i in D). As such, D becomes a normal discriminator which is *independent* along time steps. It

can be seen from the the right column of each example in Figure 10 that the temporal coherence becomes even worse when further removing the m_i condition in D . Similar result can also be observed from the quantitative and MOS results in Figure 11. These results indicate that the long-term and short-term temporal conditions h_i^D and m_i are effective to facilitate D to judge raw and compressed videos according to temporal coherence, in addition to the spatial texture. This way, it is able to force G to generate temporally coherent and visually pleasing video, thus resulting in good perceptual quality. The video examples of ablation models are provided in the project page.

Note that, in Figure 11, the MOS values of PLVC (w/o h_i^D) and PLVC (w/o h_i^D , w/o m_i in D) are even lower than PLVC (w/o GAN) at some bit-rates. This is probably because the incoherent frames generated by PLVC without temporal conditions h_i^D and/or m_i severely degrade the perceptual quality, making their perceptual quality even worse than the distortion-optimized model.

Conclusion

This paper has proposed a recurrent GAN-based perceptual video compression approach. In our approach, the recurrent generator learns to compress video with coherent and visually pleasing frames to fool the recurrent discriminator, which learns to judge the raw and compressed videos conditioned on spatial-temporal features. An adversarial loss function is designed to train the proposed model towards perceptual quality. The numerical results and user studies both validate the outstanding perceptual performance of the proposed method, compared with the latest traditional standard HM 16.20 and learned video compression methods.

References

- Agustsson, E.; Minnen, D.; Johnston, N.; Balle, J.; Hwang, S. J.; and Toderici, G. 2020. Scale-space flow for end-to-end optimized video compression. In *Proceedings of the IEEE/CVF Conference on Computer Vision and Pattern Recognition (CVPR)*, 8503–8512.
- Agustsson, E.; Tschannen, M.; Mentzer, F.; Timofte, R.; and Gool, L. V. 2019. Generative adversarial networks for extreme learned image compression. In *Proceedings of the IEEE International Conference on Computer Vision (ICCV)*, 221–231.
- Ballé, J.; Laparra, V.; and Simoncelli, E. P. 2017. End-to-end optimized image compression. In *Proceedings of the International Conference on Learning Representations (ICLR)*.
- Ballé, J.; Minnen, D.; Singh, S.; Hwang, S. J.; and Johnston, N. 2018. Variational image compression with a scale hyperprior. In *Proceedings of the International Conference on Learning Representations (ICLR)*.
- Bellard, F. 2018. BPG Image Format. <https://bellard.org/bpg/>.
- Bińkowski, M.; Sutherland, D. J.; Arbel, M.; and Gretton, A. 2018. Demystifying MMD GANs. In *Proceedings of the International Conference on Learning Representations (ICLR)*.
- Bossen, F. 2013. Common test conditions and software reference configurations. *JCTVC-L1100*, 12.
- Cheng, Z.; Sun, H.; Takeuchi, M.; and Katto, J. 2019. Learning Image and Video Compression through Spatial-Temporal Energy Compaction. In *Proceedings of the IEEE Conference on Computer Vision and Pattern Recognition (CVPR)*, 10071–10080.
- Choi, Y.; El-Khamy, M.; and Lee, J. 2019. Variable rate deep image compression with a conditional autoencoder. In *Proceedings of the IEEE/CVF International Conference on Computer Vision (ICCV)*, 3146–3154.
- Cisco. 2020. Cisco Annual Internet Report (2018–2023) White Paper. <https://www.cisco.com/c/en/us/solutions/collateral/service-provider/visual-networking-index-vni/white-paper-c11-738429.html>.
- Djelouah, A.; Campos, J.; Schaub-Meyer, S.; and Schroers, C. 2019. Neural inter-frame compression for video coding. In *Proceedings of the IEEE/CVF International Conference on Computer Vision (ICCV)*, 6421–6429.
- Golinski, A.; Pourreza, R.; Yang, Y.; Sautiere, G.; and Cohen, T. S. 2020. Feedback recurrent autoencoder for video compression. In *Proceedings of the Asian Conference on Computer Vision (ACCV)*.
- Goodfellow, I. J.; Pouget-Abadie, J.; Mirza, M.; Xu, B.; Warde-Farley, D.; Ozair, S.; Courville, A. C.; and Bengio, Y. 2014. Generative Adversarial Nets. In *Proceedings of the Advances in Neural Information Processing Systems (NeurIPS)*.
- He, D.; Zheng, Y.; Sun, B.; Wang, Y.; and Qin, H. 2021. Checkerboard Context Model for Efficient Learned Image Compression. In *Proceedings of the IEEE/CVF Conference on Computer Vision and Pattern Recognition (CVPR)*, 14771–14780.
- Heusel, M.; Ramsauer, H.; Unterthiner, T.; Nessler, B.; and Hochreiter, S. 2017. GANs trained by a two time-scale update rule converge to a local nash equilibrium. In *Proceedings of the Advances in Neural Information Processing Systems (NeurIPS)*.
- Hu, Y.; Yang, W.; and Liu, J. 2020. Coarse-to-Fine Hyper-Prior Modeling for Learned Image Compression. In *Proceedings of the AAAI Conference on Artificial Intelligence*.
- Hu, Z.; Chen, Z.; Xu, D.; Lu, G.; Ouyang, W.; and Gu, S. 2020. Improving deep video compression by resolution-adaptive flow coding. In *Proceedings of the European Conference on Computer Vision (ECCV)*, 193–209. Springer.
- Johnston, N.; Vincent, D.; Minnen, D.; Covell, M.; Singh, S.; Chinen, T.; Jin Hwang, S.; Shor, J.; and Toderici, G. 2018. Improved lossy image compression with priming and spatially adaptive bit rates for recurrent networks. In *Proceedings of the IEEE Conference on Computer Vision and Pattern Recognition (CVPR)*, 4385–4393.
- Lee, J.; Cho, S.; and Beack, S.-K. 2019. Context-adaptive entropy model for end-to-end optimized image compression. In *Proceedings of the International Conference on Learning Representations (ICLR)*.
- Lin, J.; Liu, D.; Li, H.; and Wu, F. 2020. M-LVC: multiple frames prediction for learned video compression. In *Proceedings of the IEEE/CVF Conference on Computer Vision and Pattern Recognition (CVPR)*, 3546–3554.
- Liu, H.; Huang, L.; Lu, M.; Chen, T.; and Ma, Z. 2020. Learned Video Compression via Joint Spatial-Temporal Correlation Exploration. In *Proceedings of the AAAI Conference on Artificial Intelligence*.
- Lu, G.; Cai, C.; Zhang, X.; Chen, L.; Ouyang, W.; Xu, D.; and Gao, Z. 2020. Content adaptive and error propagation aware deep video compression. In *Proceedings of the European Conference on Computer Vision (ECCV)*, 456–472. Springer.
- Lu, G.; Ouyang, W.; Xu, D.; Zhang, X.; Cai, C.; and Gao, Z. 2019. DVC: An end-to-end deep video compression framework. In *Proceedings of the IEEE Conference on Computer Vision and Pattern Recognition (CVPR)*, 11006–11015.
- Lucic, M.; Kurach, K.; Michalski, M.; Gelly, S.; and Bousquet, O. 2018. Are GANs Created Equal? A Large-Scale Study. In *Proceedings of the Advances in Neural Information Processing Systems (NeurIPS)*.
- Ma, H.; Liu, D.; Yan, N.; Li, H.; and Wu, F. 2020. End-to-End Optimized Versatile Image Compression With Wavelet-Like Transform. *IEEE Transactions on Pattern Analysis and Machine Intelligence*.
- Mentzer, F.; Agustsson, E.; Tschannen, M.; Timofte, R.; and Van Gool, L. 2018. Conditional probability models for deep image compression. In *Proceedings of the IEEE Conference on Computer Vision and Pattern Recognition (CVPR)*, 4394–4402.
- Mentzer, F.; Toderici, G. D.; Tschannen, M.; and Agustsson, E. 2020. High-Fidelity Generative Image Compression. *Proceedings of the Advances in Neural Information Processing Systems (NeurIPS)*, 33.

- Mercat, A.; Viitanen, M.; and Vanne, J. 2020. UVG dataset: 50/120fps 4K sequences for video codec analysis and development. In *Proceedings of the 11th ACM Multimedia Systems Conference*, 297–302.
- Minnen, D.; Ballé, J.; and Toderici, G. D. 2018. Joint autoregressive and hierarchical priors for learned image compression. In *Advances in Neural Information Processing Systems (NeurIPS)*, 10771–10780.
- Mirza, M.; and Osindero, S. 2014. Conditional generative adversarial nets. *arXiv preprint arXiv:1411.1784*.
- Miyato, T.; Kataoka, T.; Koyama, M.; and Yoshida, Y. 2018. Spectral Normalization for Generative Adversarial Networks. In *Proceedings of the International Conference on Learning Representations (ICLR)*.
- Ranjan, A.; and Black, M. J. 2017. Optical flow estimation using a spatial pyramid network. In *Proceedings of the IEEE Conference on Computer Vision and Pattern Recognition (CVPR)*, 4161–4170.
- Toderici, G.; O’Malley, S. M.; Hwang, S. J.; Vincent, D.; Minnen, D.; Baluja, S.; Covell, M.; and Sukthankar, R. 2016. Variable Rate Image Compression with Recurrent Neural Networks. In *Proceedings of the International Conference on Learning Representations (ICLR)*.
- Toderici, G.; Vincent, D.; Johnston, N.; Jin Hwang, S.; Minnen, D.; Shor, J.; and Covell, M. 2017. Full resolution image compression with recurrent neural networks. In *Proceedings of the IEEE Conference on Computer Vision and Pattern Recognition (CVPR)*, 5306–5314.
- Wang, Z.; Simoncelli, E. P.; and Bovik, A. C. 2003. Multi-scale structural similarity for image quality assessment. In *Proceedings of The Thirty-Seventh Asilomar Conference on Signals, Systems & Computers, 2003*, volume 2, 1398–1402. IEEE.
- Wu, C.-Y.; Singhal, N.; and Krahenbuhl, P. 2018. Video compression through image interpolation. In *Proceedings of the European Conference on Computer Vision (ECCV)*, 416–431.
- Xu, D.; Lu, G.; Yang, R.; and Timofte, R. 2020. Learned image and video compression with deep neural networks. In *Proceedings of the IEEE International Conference on Visual Communications and Image Processing (VCIP)*, 1–3. IEEE.
- Xue, T.; Chen, B.; Wu, J.; Wei, D.; and Freeman, W. T. 2019. Video enhancement with task-oriented flow. *International Journal of Computer Vision*, 127(8): 1106–1125.
- Yang, R.; Mentzer, F.; Gool, L. V.; and Timofte, R. 2020. Learning for video compression with hierarchical quality and recurrent enhancement. In *Proceedings of the IEEE/CVF Conference on Computer Vision and Pattern Recognition (CVPR)*, 6628–6637.
- Yang, R.; Mentzer, F.; Van Gool, L.; and Timofte, R. 2021. Learning for video compression with recurrent auto-encoder and recurrent probability model. *IEEE Journal of Selected Topics in Signal Processing*, 15(2): 388–401.
- Zhang, R.; Isola, P.; Efros, A. A.; Shechtman, E.; and Wang, O. 2018. The unreasonable effectiveness of deep features as a perceptual metric. In *Proceedings of the IEEE Conference on Computer Vision and Pattern Recognition (CVPR)*, 586–595.

Perceptual Learned Video Compression with Recurrent Conditional GAN

– Supplementary Material –

Ren Yang, Luc Van Gool, Radu Timofte

Computer Vision Laboratory, D-ITET, ETH Zurich, Switzerland

Detailed architectures

Figure 12 shows the detailed architecture of the recurrent generator G . In Figure 12, the convolutional layers are denoted as “Conv, filter size, filter number”. GDN (Ballé, Laparra, and Simoncelli 2017) and ReLU are the activation functions. Note that the layers with ReLU before Conv indicates the pre-activation convolutional layers. $\downarrow 2$ and $\uparrow 2$ are $\times 2$ downscaling and upscaling, respectively. In the quantization layer, we use the differentiable quantization method proposed in (Ballé, Laparra, and Simoncelli 2017) when training the models, and use the rounding quantization for test. The Convolutional LSTM (ConvLSTM) layers in the auto-encoders make the proposed G have the recurrent structure.

The detailed architecture of the proposed recurrent conditional discriminator D is illustrated in Figure 13. The denotations are the same as Figure 12. In D , we utilize the spectral normalization (Miyato et al. 2018), which has been proved to be beneficial for discriminator. In the leaky ReLU, we set the leaky slope as 0.2 for negative inputs. Finally, the sigmoid layer is applied to output the probability in the range of $[0, 1]$.

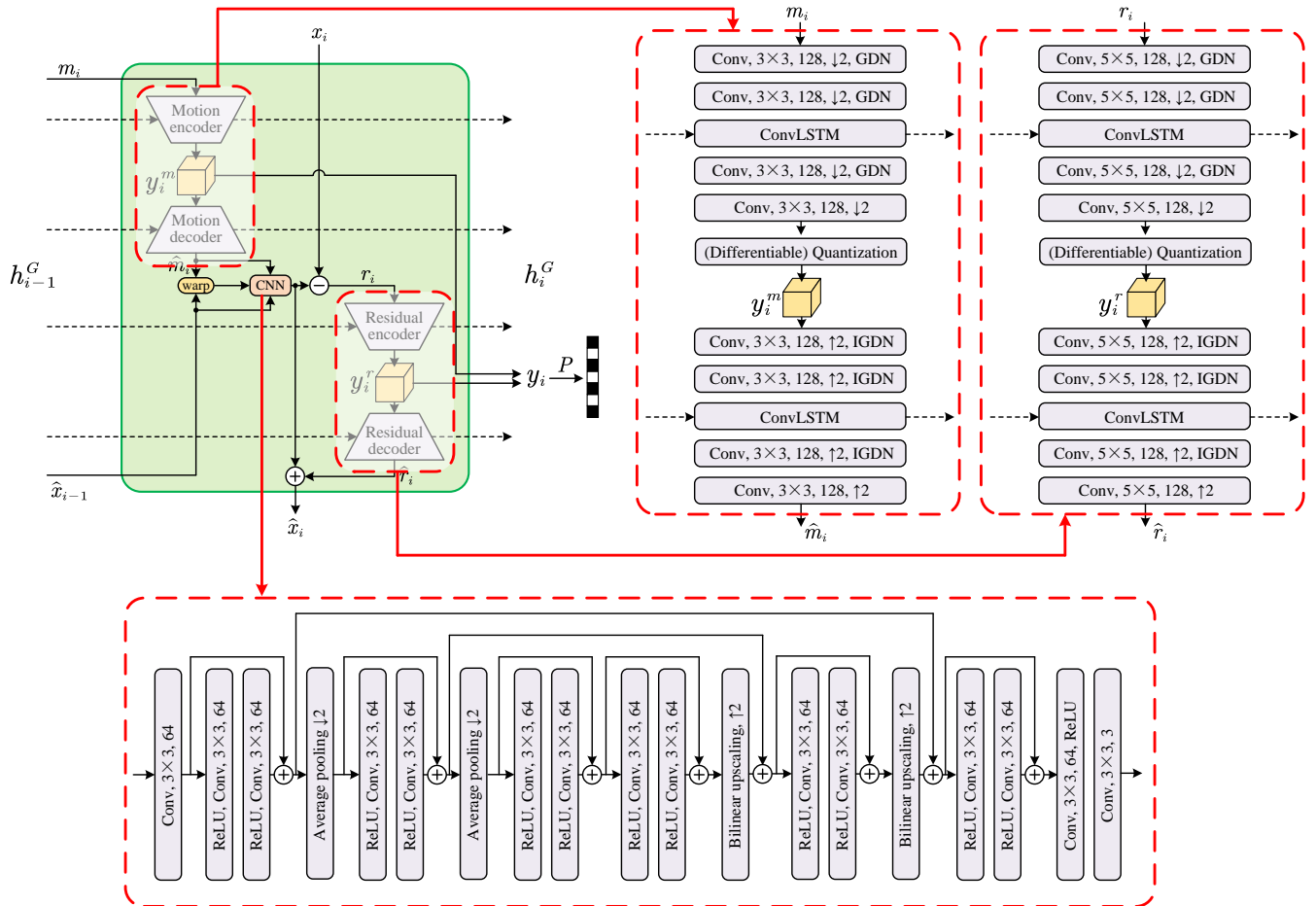


Figure 12: The detailed architecture of the recurrent generator G .

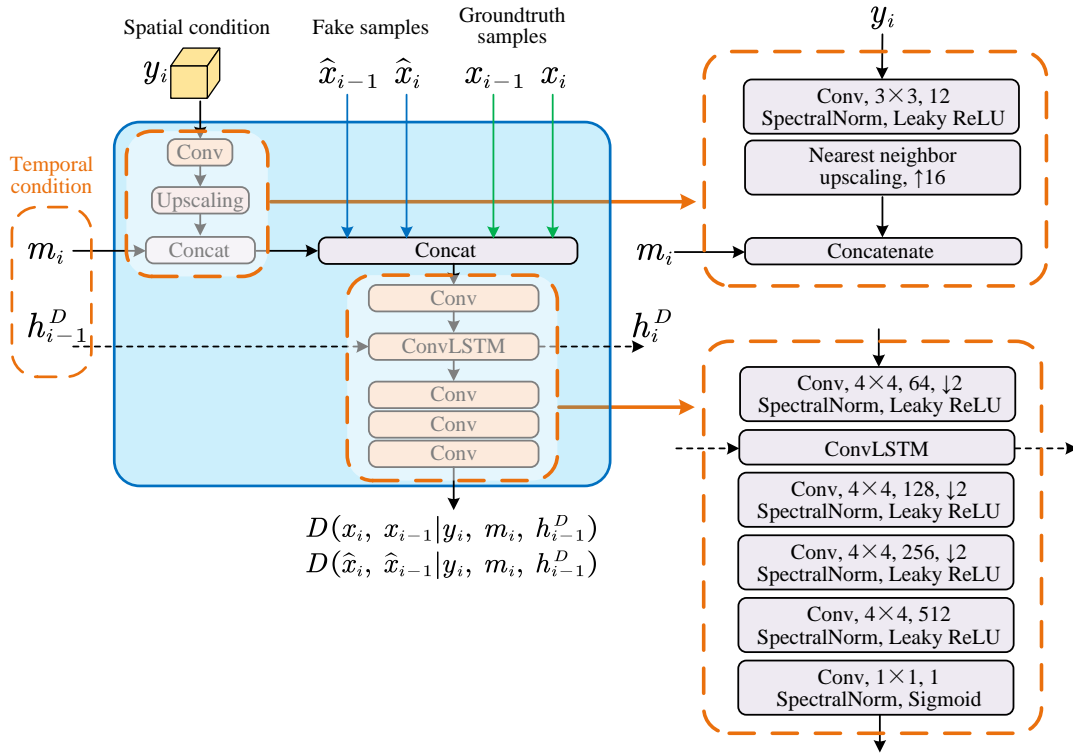


Figure 13: The detailed architecture of the recurrent conditional discriminator D .

Standard deviation of MOS performance

Recall that we conducted a user study to evaluate the perceptual performance of ours and compared methods in Figure 8. To further study into the MOS values, we calculate the standard deviation of MOS values among all raters, and show the results along bit-rates in Figure 14. It can be seen from Figure 14 that the standard deviation of MOS values of our PLVC approach is relatively lower than HM 16.20 and RLVC (Yang et al. 2021). This indicates that the proposed PLVC models achieve more stable perceptual quality than other methods. In another word, the subjects tend to consistently admire the better perceptual quality of our approach, in comparison with HM 16.20 and RLVC (Yang et al. 2021).

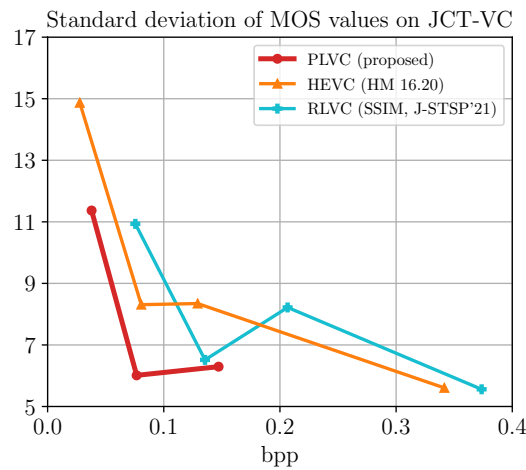


Figure 14: The standard deviation of MOS values on the JCT-VC dataset.

Visual results

We illustrate more visual results in Figure 15 (on the *last* page), which shows both spatial textures and temporal profiles of the proposed PLVC approach, HEVC (HM 16.20) and RLVC (MS-SSIM) (Yang et al. 2021), in addition to Figure 6 in the main text. It can be seen from Figure 15, the proposed PLVC approach achieves more detailed and sharp textures than other methods, even if when HEVC consumes obviously more bit-rates and RLVC consumes more than $2\times$ bits. Besides, the temporal profiles also show that our PLVC approach has similar temporal coherence to the groundtruth, and the temporal profiles also show that we generate more photo-realistic textures than the compared methods. These results are consistent with the user study in Figure 8 of the main text, validating the outstanding perceptual performance of the proposed PLVC approach.

Video example

We will provide the video examples for a better visual comparison at the project page <https://github.com/RenYang-home/PLVC>.

Computing platform and codes

We conduct all training and test procedures on a group of TITAN Xp GPUs with Debian GNU/Linux 10 system. We will publicly release all codes with pre-trained models on the project page.

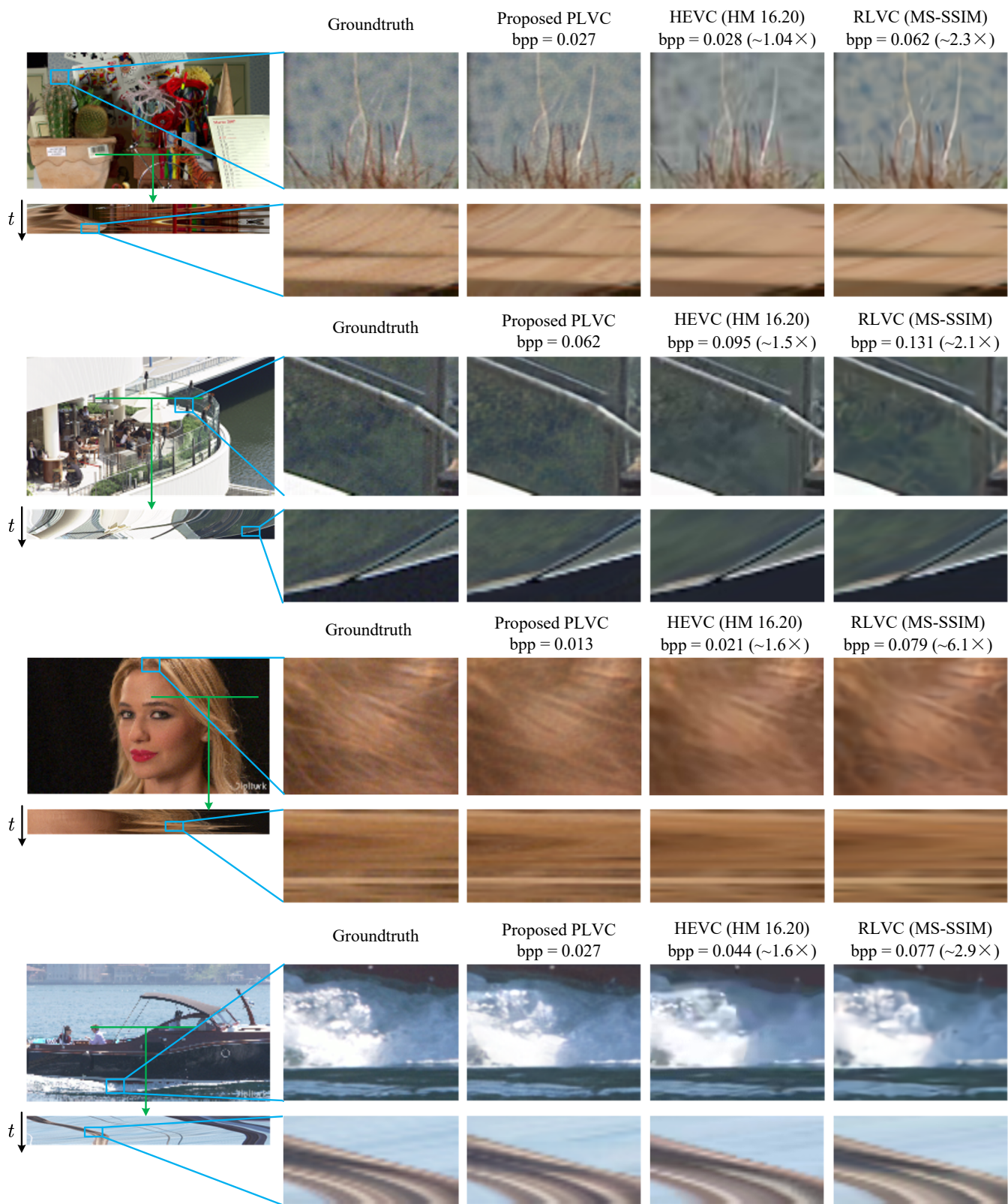


Figure 15: The visual results of the proposed PLVC approach in comparison with HM 16.20 and the MS-SSIM optimized RLVC *et al.* (Yang *et al.* 2021)